HHS Public Access

Author manuscript

Science. Author manuscript; available in PMC 2020 February 22.

Published in final edited form as:

Science. 2019 February 22; 363(6429): 838–845. doi:10.1126/science.aav5606.

Scalable and safe synthetic organic electroreduction inspired by Li-ion battery chemistry

Byron K. Peters[1,†], **Kevin X. Rodriguez**[1,†], **Solomon H. Reisberg**[1], **Sebastian B. Beil**[1], **David P. Hickey**[4], **Yu Kawamata**[1], **Michael Collins**[2], **Jeremy Starr**[2], **Longrui Chen**[3], **Sagar Udyavara**[5], **Kevin Klunder**[4], **Timothy Gorey**[4], **Scott L. Anderson**[4], **Matthew Neurock**[5,*], **Shelley D. Minteer**[4,*], **Phil S. Baran**[1,*]

[1]Department of Chemistry, Scripps Research, 10550 North Torrey Pines Road, La Jolla, CA 92037, USA.

[2]Discovery Sciences, Medicine Design, Pfizer Global Research and Development, 445 Eastern Point Road, Groton, CT 06340, USA.

[3]Asymchem Life Science (Tianjin), Tianjin Economic-Technological Development Zone, Tianjin 300457, China.

[4]Department of Chemistry, University of Utah, Salt Lake City, UT 84112, USA.

[5]Department of Chemical Engineering and Materials Science, University of Minnesota, Minneapolis, MN 55455, USA.

Abstract

Reductive electrosynthesis has faced long-standing challenges in applications to complex organic substrates at scale. Here, we show how decades of research in lithium ion battery materials, electrolytes, and additives can serve as an inspiration for achieving practically-scalable reductive electrosynthetic conditions for the Birch reduction. Specifically, we demonstrate that using a sacrificial anode material (Mg or Al), combined with a cheap, non-toxic, and water-soluble proton source (dimethylurea), and an overcharge protectant inspired by battery technology (tris(pyrrolodino)phosphoramide) can allow for multigram-scale synthesis of pharmaceutically-relevant building blocks. We show how these conditions have an exceptional level of functional-

*Corresponding author. pbaran@scripps.edu (P.S.B.), minteer@chem.utah.edu (S.D.M.), mneurock@umn.edu (M.N.).

Author contributions:

B.K.P and P.S.B conceived of the project. B.K.P., K.X.R., S.H.R., S.B.B., D.P.H., Y.K., M.C., J.S., S.U., K.K., T.C., S.L.A., M.N., S.D.M., and P.S.B designed the experiments. B.K.P., K.X.R., S.H.R., S.B.B., D.P.H, L.C., S.U., and K.K. ran the experiments. B.K.P., K.X.R., S.H.R., S.B.B., D.P.H., Y.K., M.C., J.S., S.U., K.K., T.C., S.L.A., M.N., S.D.M., and P.S.B analyzed the data. B.K.P, K.X.R., S.H.R., D.P.H., S.U., M.N, S.D.M., and P.S.B. wrote the manuscript.

†B.K.P and K.X.R contributed equally to this work.

Competing interests: P.S.B. serves on a scientific advisory panel for Asymchem.

Data and materials availability: Detailed experimental and analytical procedures and full spectral data is available in the Supplementary Materials.

Supplementary Materials:
Materials and Methods
Supplementary text
Figs. S1–83
Tables S1–7
References (61–112)
NMR Spectra

group tolerance relative to classical electrochemical and chemical dissolving metal reductions. Finally, we demonstrate that the same electrochemical conditions can be applied to other dissolving-metal-type reductive transformations, including McMurry couplings, reductive ketone deoxygenations, and reductive epoxide openings.

One Sentence Summary:

Safe and scalable access to synthetically-useful strongly reducing species, usually only available via dissolving metals in amine solvents, is accomplished using a convenient electrolyte system in an electrochemical process reminiscent of Li-ion battery technology.

The use of alkali metals as reagents for strongly reductive chemistry has found limited use in the modern era due to safety considerations and immense difficulty in industrial scale-up. The Birch reduction, a flagship example, is one of the first reactions taught in undergraduate organic chemistry lectures(1) for the rapid access it affords to sp^3 complexity from simple feedstock arenes.(2–5) Yet typical procedures call for the hazardous condensation of ammonia, or other volatile amines, as solvent, combined with pyrophoric metals at cryogenic temperatures. Milder alternatives have been reported that rely on finely-dispersed silica-impregnated Na (SiGNa-S1) and Na/K(6–8) or various mineral oil dispersions combined with superstoichiometric amounts of an expensive/toxic crown ether additive.(9, 10) However, these reagents either fail to access the same reactivity space as, for example, Li/NH_3, or still require extreme caution in reaction setup on account of the alkali metal. Perhaps the most compelling modern Birch application stems from Pfizer's kilogram-scale synthesis of the anti-Parkinson's drug candidate, sumanirole (**2**, Fig. 1A).(11) The tandem aziridine opening/debenzylation of the direct precursor **1** is a remarkable achievement in process chemistry and engineering that required the use of custom equipment to administer lithium metal, and enough ammonia to fill three Boeing 747 airliners in the gas phase. At the end of the reaction, which was conducted at cryogenic temperature (−35 °C), 2300 L of H_2 were liberated — an understandably intimidating occurrence.

In this context, electrochemical reduction is an appealing alternative. Indeed, several groups have explored the idea of electrochemical surrogates for alkali metal reductions (Fig. 1B and C)(12–14) with a key report by Kashimura demonstrating proof-of-concept for electrochemically-driven Birch reactivity.(15) Nonetheless, electrochemical reductions have been hindered by a myriad of unwanted side-reactions that typically overpower the desired reactivity, including competing proton reduction, electrode passivation from excessive electrolysis of solvent, and diminished yields caused by adventitious O_2. Perhaps most telling, to synthesize **2** on process scale, Pfizer utilized chemical Birch over any then-known electrochemical alternatives. *For Pfizer, a kilogram-scale chemical Birch reduction was more practical to scale than any electrochemical method*, despite the enormous engineering challenges associated with the former. Corroborating these limitations, in our hands, attempts to reduce **1** using a variety of the known electrochemical conditions were completely fruitless (See Supplementary Materials).

Concurrent with these initial forays into electrochemical reduction, the quest to achieve a cyclable, safe, and high energy density Li-ion battery has faced similar challenges,

culminating in a better understanding of the role that additives, solvent, and electrolyte play in the formation of a solid electrolyte interphase (SEI).(16, 17) Importantly, the SEI prevents buildup of an excessive passivating layer at the electrode while enabling a more active and stable electrode interface under extreme potentials (Fig. 1D) (18, 19). Application of these concepts to Li-ion battery technology is largely responsible for their widespread use in virtually all modern electronics, including smart phones, laptops, and electric vehicles. Inspired by this transformative technology, we sought to optimize electroorganic synthesis using the approaches originally developed for Li-ion batteries.(20) We show herein that such strongly reducing conditions can thereby be accessed in a simple and safe way, at ambient temperature without rigorous exclusion of air or moisture and can be applied to the most popular reaction classes in this arena such as Birch, debenzylation, epoxide/aziridine opening, and McMurry couplings.

Electrochemistry represents a convenient way to precisely select redox potentials for use in organic synthesis. Anodic, or oxidative, processes constitute the vast majority of commonly-employed electrochemical transformations, and run the gamut of C–H oxidation,(21) decarboxylation,(22) oxidative couplings,(23, 24) and olefin functionalizations.(25, 26) In contrast, cathodic reductions(27–29) have received considerably less use in modern preparative synthesis. This lower utility is likely due to three factors: First, many reductive methods are limited to divided cells, which can seem daunting enough to frighten off prospective users, in addition to the engineering challenges they pose in setting up high throughput screenings and scale-up contexts (we note that divided cells are vitally important to preparative electrosynthesis, as they often alleviate redox incompatibilities/mismatches incurred in undivided cells, but with their complex construction, adoption from the broader synthetic community has been limited). Second, most electroreductive methods rely on a mercury pool cathode, a technique with extreme health and safety repercussions. Finally, while there are examples of other reductive electrosyntheses in the literature which demonstrate good chemoselectivity under such reductive conditions,(30) achieving chemoselectivity for electrochemical Birch reduction in the presence of other electrophores has remained an unanswered challenge. Indeed, on approach of strongly reductive conditions (including those required to access Li^0), most common electrolytes disintegrate.(31, 32) Thus, while accessing this extreme reactivity using cathodic reduction is not a new idea, accessing it in a way that is both *practical and scalable* is a goal that has not been achieved. Birch himself reported the first electrochemically-mediated arene reduction of toluene (with $NaOEt/NH_3$).(33) Additional reports following up on that pioneering study have appeared, including the key report by Kashimura (*vide supra* and Fig. 1C). However, all of them exhibit narrow scopes — Kashimura's method is limited to hydrocarbons — and they require procedures (e.g., continuous sonication) that are no more scalable than a purely chemical Birch. (12, 13, 15, 34–47)

Li-ion battery interphase design applied to electroreduction

Accordingly, the current study began with an extensive evaluation of this prior art (partial results in Fig. 1E; for a complete listing, see Supplementary Materials), of which select efforts are summarized in entries 1–4.(12, 13, 15, 36, 42, 43, 48) To help probe the functional-group tolerance of these prior works, we opted for phenyl ethanol (**3**) as a model

substrate. The conditions reported by Kashimura(15) were chosen as a basis set from which to launch more extensive optimization (entry 4); however, the limitations of that state-of-the-art were clearly demonstrated in that **3**'s alcohol moiety completely shut down reactivity under Kashimura's conditions. To optimize, $LiClO_4$ was first replaced with LiBr due to the bromide salt's higher stability, affordability, and similar range of solubility; however, only trace product was detected (entry 5). An accumulation of an apparently metallic substance at the cathode reacted violently with MeOH and water during cleaning, and so provided an initial clue for further study. We reasoned that this material was Li metal that had reductively plated out due to the poor solubility of Li^0 in THF. Indeed, similar events were observed in the early days of Li-ion battery exploration as a result of battery overcharging.(49) To combat this problem, several additives similar to those known for dampening the effects of overcharging in Li-ion batteries (including glyme, dioxane, and phosphoramides; see Supplementary Materials for complete list) were evaluated, with tris(pyrrolidino)phosphoramide (TPPA), a non-carcinogenic surrogate for HMPA,(50) emerging as optimal (entry 6). Although the desired product was observed in 50% yield, it was accompanied by undesired isomers and over-reduced species in *ca.* 30% yield. Unsurprisingly, varying the proton source had a profound effect on the distribution of these compounds. After an extensive screen (See Supplementary Materials), we determined that 1,3-dimethylurea (DMU) was the most selective for the desired product (entry 7). As expected, reduced temperature afforded greater selectivity (entry 8). Consistent with Kashimura's findings,(15) it was found that switching from an Al to a Mg anode and increasing the current density on the cathode (by decreasing its surface area) rendered the reaction more selective and efficient at room temperature (entry 9). It is postulated that the anode is sacrificially oxidized, and it is possible that the identity of the resultant oxidized metal salts is relevant to the observed reactivity (*vide infra).*

Mechanistic investigation

Electroanalytical and computational study of reaction kinetics

With an optimized set of conditions in hand, the intriguing mechanism of transformation was explored in a variety of contexts. Intuitively, one may assume that the cathode simply generates Li^0 species (whether homogeneous, heterogeneous, or electroplated) that are responsible for the observed reactivity, which in turn implies that electrolysis could be decoupled from the actual substrate reduction. To test this hypothesis, a degassed reaction solution — with the substrate and DMU omitted — was electrolyzed as normal, under an inert atmosphere at −78 °C, to putatively accumulate electrochemically-generated Li^0 species.(51) After electrolysis was completed (1.5 hours, 5 F/mol), the substrate was then added, and the reaction was stirred, with samples drawn at 30-minute intervals (Fig. 2A). There was a small decrease in the substrate concentration over time, but no desired product or well-defined side products could be detected during this time. Similar trends held true for an analogous experiment run at room temperature (see Supplementary Materials). The apparent disconnect between putative Li^0 generation, and lack of Birch reactivity, strongly suggested that a typical Li^0 species is not the active reductant in our reaction manifold. We hypothesized that instead, arene substrate was getting reduced directly on the electrode

surface. To probe this hypothesis, we underwent a variety of computational and electroanalytical experiments.

First, *ab initio* calculations (see Supplementary Materials for detailed methods) were undertaken (Fig. 2B) to compare the kinetics of the solution-phase reduction of **3** via Li^0 species (red path, top) to the kinetics of **3**'s direct reduction at the electrode surface at −2.25V *vs.* NHE (blue path, bottom). The reduction of **3** via the Li-mediated path is predicted to proceed initially *via* electron transfer from the lithium metal (Li^0) to **3**, forming the anion radical **3a** and generating the lithium cation (Li^+); **3a** is then protonated in the solution phase *via* DMU to form the radical intermediate (**3b**). This first protonation step, as shown in Fig. 2B, is the highest energy state along the path with an activation barrier of 52 kJ/mol. On the other hand, the electrode-mediated pathway began with **3**'s adsorption to the cathode, followed by an electron transfer event from the cathode, to generate adsorbed radical anion ($\mathbf{3a^{ads}}$). Both adsorption and the heterogeneous electron transfer were calculated to be barrierless. Facile protonation of $\mathbf{3a^{ads}}$ resulted in the formation of the adsorbed radical $\mathbf{3b^{ads}}$, which could undergo a second barrierless electrode-to-substrate electron transfer to give the adsorbed anion ($\mathbf{3c^{ads}}$). Finally, the rate-determining protonation gave the adsorbed diene $\mathbf{4^{ads}}$ with a calculated barrier of 41 kJ/mol. Facile desorption was calculated to give the solution-phase product (**4**). Comparing the two pathways, these computations clearly support superior kinetic facility of an on-electrode reductive mechanism, rather than one mediated by Li^0.

To further investigate reaction kinetics, the reaction was monitored (*via* GC/MS analysis of quenched aliquots) under standard electrochemical conditions at five-minute intervals (Fig. 2C, left). Essentially no induction period was observed, and no competitive processes were detected based on the absence of side-products. Furthermore, analysis suggests zero-order kinetics in substrate: Consumption of phenyl ethanol **3** and formation of product were both well-fitted by linear regression ($r^2 = 0.99$ and 0.98, respectively). The slight deviation from linearity observed is likely due to the small dataset collected. We also studied the reaction rate's dependence on current (Fig. 2C, right). A clear positive correlation between current and rate was observed; we attempted to determine the rate order *via* Jordi-Burés plot(52). While a first-order plot was the closest fit to the data (Fig 2C, right inset), the fit was not perfect, suggesting that the rate's dependence on current is quite complex. Nonetheless, the rate order is clearly positive. Taken together, these data are consistent with a kinetic picture in which electron flow from the cathode is rate-limiting, rather than any chemical transformation.

While voltammetric studies on the electrochemical reduction of arenes have been performed by others, the focus of these precedents' was on polyaromatics as electron shuttles/ mediators/catalysts rather than substrates, and thus did not elucidate the details of protonation and second electron transfer events.(53) We thus sought out to study the microscopic electrochemical steps using a combination of voltammetric techniques (Fig. 3). We initially hoped to use **3** as a model to study. Unfortunately, however, under very similar conditions to our preparative reduction, lithium alkoxides are electrochemically generated at potentials higher (less negative) than that of **3**, thereby obfuscating critical details of the electron transfer steps. Under the general assumption that a given mechanism (or set of

mechanisms) is common to all substrates, our focus shifted to naphthalene **5** as a model substrate for voltammetric analysis under our optimized reaction conditions. Variable frequency square wave voltammetry (SWV) of **5** (Fig. 3A) indicated two distinguishable electrochemical reduction steps that are resolved at high frequencies (i.e. some Electron-transfer, Electron-transfer; EE process). This result is consistent with a mechanism involving direct reduction of **5** at the electrode. It should be noted that this two-electron transfer could either occur consecutively prior to two subsequent protonation steps (Electron-transfer, Electron-transfer, Chemical-protonation, Chemical-protonation; EECC mechanism) or with a chemical step separating them (Electron-transfer, Chemical-protonation, Electron-transfer, Chemical-protonation; ECEC mechanism). To differentiate between these possibilities, we utilized cyclic voltammetry (see Supplementary Materials), the results of which revealed that varying the CV potential window had an influence on the reversibility of the scan. This is inconsistent with an EE mechanism and is evidence that these two processes are separated by a chemical step (protonation) prompting us to invoke an ECEC mechanism (refer to Supplementary Materials for more in-depth discussion). While elements of the data are also consistent with a DISP-type mechanism, the zero-order kinetics in substrate (*vide supra*) is not. Thus, an ECEC type mechanism seems most likely.

Notably, these CV experiments also demonstrated that without LiBr, the scans showed good reversibility, highlighting the crucial role of Li^+ in guiding the reaction toward the product. Combining this insight with DMU's unique superiority (See Supplementary Materials for other proton sources screened) as a proton donor, we probed the possible interaction between Li^+ and DMU *via* attenuated total reflectance (ATR, Fig. 3B). We observed a complete, quantitative shift in the C=O stretching frequency of DMU from 1620 cm^{-1} to 1660 cm^{-1} in the absence and presence of LiBr, respectively, which provides strong evidence for a Li^+/DMU complexation.

Taken together, all of these results are consistent with a mechanism involving sequential electrode-mediated single-electron reduction, protonation, additional electrode-mediated reduction and a final protonation (Fig. 3C). The unique ability of Li^+ to form a relatively strong coordinative complex to DMU may be critical to colocalize DMU and **5b** (Fig. 3D, top). To support this hypothesis for Li^+'s role in the reaction manifold, we attempted control experiments with NaBr and KBr in place of LiBr. While no reaction was observed, these salts' inherent insolubility dramatically altered the resistivity of the solution, and thus thwarted direct comparisons to the LiBr system. More soluble surrogates of these non-lithium cations, such as NaI, nonetheless did not afford any product.

Regardless of the nuanced role of Li^+ in the reaction, these studies conclusively showed that Li^0 does not play a role as a direct solution-phase arene reductant. Furthermore, on treating a pre-electrolyzed LiBr solution (at −78 °C) with a more reductively labile aldehyde, we did not observe any of the reduced alcohol or pinacol products (see Figure 2A and Supplementary Materials). This data rules out the mechanistic possibility of solvated electrons as the active reductant. Preliminary investigations into the rate laws of the reaction show a complicated kinetic picture where multiple pathways may be operative; more detailed studies on the mechanism and kinetics of this reaction manifold are ongoing in our laboratories.

Electrode surface interrogation

The addition of TPPA to the **5**/DMU/LiBr solution does not result in the increased electron transfer rates that would be expected of electrochemical mediation through $Li^{+/0}$. This suggests that the role of TPPA may not be intrinsically tied to the mechanistic cycle, but rather may be involved in ancillary electrochemical processes (Fig. 3C). Structurally similar molecules (such as HMPA) have been employed in Li-ion batteries to aid in dissolving Li_2O layers formed at the electrode interface.(54) With this in mind, the unique speciation at the electrode surface was interrogated using X-ray photoelectron spectroscopy (XPS).

In general, a major problem with electroorganic synthesis under extreme reductive potentials is the formation of thick passivation layers on the electrode surface that inhibit product formation and lead to extensive side products. Evidence of this passivation in our system was demonstrated in the absence of TPPA, as shown in the Supplementary Materials. Although optimized conditions still evidenced a thin film on the electrode surface (see Supplementary Materials), this film ceased to grow within minutes and appeared to stabilize along the working electrode. XPS analysis revealed Mg, P, N and large amounts of lithium deposited on the electrode surface, as well as increased levels of oxygen and carbon; detailed analysis of the spectra is provided in the Supplementary Materials. The observed Li, O, and C are likely a result of THF decomposition to form Li alkoxide.(55) Surprisingly, zinc was still observed in the post-reaction film, providing evidence that the underlying electrode material is still accessible to the bulk solution. The film may also be involved in both forming a stable SEI and providing an active electrode surface for the reaction. Although the exact mechanism of film growth and suppression are not yet known, it is clear that all system components are incorporated into the film and may cooperatively maintain electrode activity.

Finally, given our use of a sacrificial anode, and its putative generation of magnesium salts during the reaction, we also probed the possible role of anode-derived magnesium salts on the reaction mechanism. We found that addition of stoichiometric and super-stoichiometric amounts of $MgBr_2 \bullet Et_2O$ under our electrochemical protocol not only gave the desired diene **4** in a diminished yield (30% vs. 74%), but also gave an overall lower consumption of **3** (See Supplementary Materials). In addition, we observed that in the absence of stirring, diminished yields could be correlated with decreased distances between the cathode and anode, suggesting that diffusion of metal salts from the anode is deleterious to the reaction. Although we cannot fully rule out that these metallic ions are mechanistically relevant, given the deleterious nature of Mg salts to the overall reaction, we hypothesize that any exogenous salts generated under the electrochemical conditions are most likely not mechanistically critical.

Applications to complex substrates

As shown in Fig. 4, the electroreduction exhibited a broad scope across a range of different arenes. Under optimized conditions, every aryl group within a given polyarene was efficiently reduced (**6** and **7**), an achievement not accomplished by ammonia-free variants (e.g., SiGNa)(8), other dispersions(10) and more weakly reductive conditions.(56) Simple arenes proved facile (**8** and **9**), as did aryl ethers, including those with both *meta* and *para*

substituents (**10** and **11**). Silyl ethers performed well (**12** and **13**), despite their conspicuous absence from other ammonia-free alternatives. The utility of these modular intermediates is evident from the large body of literature in which they appear.(57) Consistent with reactivity of the classical Birch, alcohol and ketone-containing arenes (**4**, **14** and **15**) were reduced in good yields (accompanied by the anticipated ketone reduction). Carbamate (**16**), amide (**17**), carboxylic acid (**18**, **19**, **21**, and **22**), and silane (**23**) functionalities were also preserved in the reduction of the aryl group. Even a sterically-guarded substrate, 1,3,5-tri-^{t}butylbenzene, could be reduced efficiently (**20**). Notably, benzoic acids were furnished in moderate yields (**18** and **19**); to our knowledge, this substrate class has historically been restricted to standard Birch conditions. The operational simplicity of this chemistry is displayed in the Birch reduction of substrate **3**; when no precautions were taken to exclude air or moisture, the reaction resulted in a similar conversion (68%).

Heterocyclic arenes, which are rarely subjected to Birch reductions, proved viable substrates. Indazole (**24**), indole (**25**, **26** and **27**), carbazole (**28**), acridine (**29/30**), and quinoline (**31**) moieties could be reduced on the carbocyclic ring in preference to the heterocycle, a reactivity only possible under a few classic Birch conditions. In our hands, SiGNa-S1 failed in all the examples tested (Fig. 4), and Na-dispersion/15-crown-5 mixture gave only partial conversion with prolonged reaction times on some substrates.

The mildness of the reaction conditions was demonstrated *via* application to more complex natural products. Thus, chemo- and regioselective reduction gave access to the 1,4-dienyl derivatives of dextromethorphan (**32**), dehydroabietic acid (**33**), and estrone methyl ether (**34**). Overall, this methodology was competitive to the chemical Birch using lithium metal (see Supplementary Materials for the referenced literature comparisons)

More broadly, the chemistry of dissolving metals has been applied to a wide range of reductive transformations, including ring opening/closing,(58) protecting group removal, transition metal-mediated reactions, among others. However, due to the poor solubility of alkali metals in reductively inert solvents (e.g., THF), these reactions have required either the use of ammonia as a co-solvent or the aid of a polyaromatic hydrocarbons (PAH) to act as electron shuttles.(59) In contrast, generation of separated Li^0 atoms can be precisely controlled in electrochemical systems; as a result, the limitations associated with bulk Li metal are simply eliminated. Encouraged by this realization, we began to explore the utility of our electroreduction protocol for non-Birch reductive transformations (Fig. 5a). Ether debenzylation proceeded smoothly (**35** → **36**) without competitive reduction of the more electron rich arene (in accord with Birch guidelines). Similarly, reductive deoxygenation was accomplished on fluorenone (**37** → **38**). Reductive cyclization, similar to an approach demonstrated by Rychnovsky,(60) (**39** → **40**) was successfully achieved. Ring opening of an epoxide (**41** → **42**) was facile, as was furan ring opening (**43** → **44**). Remarkably, McMurry couplings (**45** → **46**) could also be accomplished at room temperature. Returning to the sumanirole example outlined in Fig. 1, the same transformation was readily achieved at room temperature in 2 hours (**1** → **2**, 67% yield). It is worth noting that the most practical Birch-alternatives available (SiGNa-S1 and Na-disp./15-c-5) failed to deliver any product, as did all attempts to use previously-reported electrochemical methods (See Supplementary Materials).

Finally, the scalability of the protocol was demonstrated in both batch and flow on **12** (the direct precursor to a key Pfizer intermediate), without any loss in efficiency. The modular flow setup (Fig. 5B) is simple and allows an increase in scale by several orders of magnitude in a safe and sustainable fashion. Indeed, the very same transformation could be achieved in flow on 100 g scale, without significant changes to the protocol, special anhydrous precautions, or loss in yield.

Reductive electrochemical synthesis has been an approach discussed in the literature for nearly a century. Despite its obvious conceptual appeal, adoption of preparative methods in this subfield has been extremely limited because of issues around pragmatism and chemoselectivity. Inspired by Li-ion battery technology, we have developed a general set of electrochemical reductive conditions, and demonstrated its practicality, safety, scalability, and chemoselectivity. We believe that inspiration from the fast-evolving research areas of battery technologies and electroactive materials will have an important impact in synthetic organic electrochemistry, such as the discovery of new oxidative and reductive mediators, milder access to harsh reducing agents, and for generating low-valent catalytic systems based on transition metals.

Supplementary Material

Refer to Web version on PubMed Central for supplementary material.

Acknowledgments:

We thank Wenhua Qiao for assistance in setting up scale-up reactions. We also express our thanks to Professor Donna Blackmond for assistance in interpreting the kinetics data.

Funding: Financial support for this work was provided by NSF (CCI Phase 1 grant #1740656) to Matthew Neurock, Shelley D. Minteer and Phil S. Baran. Pfizer and Asymchem. Byron Peters and Kevin Rodriguez sincerely acknowledge the Swedish Research Council (Vetenskapsrådet, VR 2017-00362) and National Institutes of Health (PA-18-586), respectively for funding their postdoc fellowships. Yu Kawamata gratefully acknowledges the Hewitt Foundation for a post-doctoral fellowship. Solomon Reisberg gratefully acknowledges an NSF GRFP (#2017237151) and a Donald and Delia Baxter Fellowship.

References

1. Rabideau PW, Marcinow Z, The Birch reduction of aromatic compounds. Org. React. (Hoboken, NJ, U. S.) 42, 222 pp (1992).
2. Rabten W, Margarita C, Eriksson L, Andersson PG, Ir-Catalyzed Asymmetric and Regioselective Hydrogenation of Cyclic Allylsilanes and Generation of Quaternary Stereocenters via the Hosomi-Sakurai Allylation. Chem. - Eur. J 24, 1681–1685 (2018). [PubMed: 29160939]
3. Peters BK et al., Enantio- and Regioselective Ir-Catalyzed Hydrogenation of Di- and Trisubstituted Cycloalkenes. J. Am. Chem. Soc 138, 11930–11935 (2016). [PubMed: 27548029]
4. Liu J et al., Regioselective Iridium-Catalyzed Asymmetric Monohydrogenation of 1,4-Dienes. J. Am. Chem. Soc 139, 14470–14475 (2017). [PubMed: 28930455]
5. Paptchikhine A, Itto K, Andersson PG, Sequential Birch reaction and asymmetric Ircatalyzed hydrogenation as a route to chiral building blocks. Chem. Commun. (Cambridge, U. K.) 47, 3989–3991 (2011).
6. Dye JL et al., Alkali Metals Plus Silica Gel: Powerful Reducing Agents and Convenient Hydrogen Sources. J. Am. Chem. Soc 127, 9338–9339 (2005). [PubMed: 15984839]
7. Nandi P et al., Alkali Metals in Silica Gel (M-SG): A New Reagent for Desulfonation of Amines. Org. Lett 10, 5441–5444 (2008). [PubMed: 18973332]

8. Costanzo MJ, Patel MN, Petersen KA, Vogt PF, Ammonia-free Birch reductions with sodium stabilized in silica gel, Na-SG(I). Tetrahedron Lett. 50, 5463–5466 (2009).
9. Li P, Guo S, Fang J, Cheng J, Preparation and application of sodium dispersions. Huaxue Shiji 18, 234–236 (1996).
10. Lei P et al., A Practical and Chemoselective Ammonia-Free Birch Reduction. Org. Lett20, 3439–3442 (2018). [PubMed: 29846078]
11. Joshi DK, Sutton JW, Carver S, Blanchard JP, Experiences with Commercial Production Scale Operation of Dissolving Metal Reduction Using Lithium Metal and Liquid Ammonia. Org. Proc. Res. & Dev 9, 997–1002 (2005).
12. Swenson KE, Zemach D, Nanjundiah C, Kariv-Miller E, Birch reductions of methoxyaromatics in aqueous solution. J. Org. Chem 48, 1777–1779 (1983).
13. Benkeser RA, Kaiser EM, An Electrochemical Method of Reducing Aromatic Compounds Selectively to Dihydro or Tetrahydro Products. J. Am. Chem. Soc 85, 2858–2859 (1963).
14. Bordeau M, Biran C, Pons P, Leger-Lambert MP, Dunogues J, The electrochemical reductive trimethylsilylation of aryl chlorides: a good route to aryltrimethylsilanes and a novel route to tris(trimethylsilyl)cyclohexadienes. J. Org. Chem 57, 4705–4711 (1992).
15. Ishifune M et al., Electroreduction of aromatics using magnesium electrodes in aprotic solvents containing alcoholic proton donors. Electrochim. Acta 48, 2405–2409 (2003).
16. Goodenough JB, Park K-S, The Li-Ion Rechargeable Battery: A Perspective. Journal of the American Chemical Society 135, 1167–1176 (2013). [PubMed: 23294028]
17. Goodenough JB, Kim Y, Challenges for Rechargeable Li Batteries. Chemistry of Materials 22, 587–603 (2010).
18. Peled E, Menkin S, Review-SEI: Past, Present and Future. J. Electrochem. Soc 164, A1703–A1719 (2017).
19. Haregewoin AM, Wotango AS, Hwang B-J, Electrolyte additives for lithium ion battery electrodes: progress and perspectives. Energy Environ. Sci 9, 1955–1988 (2016).
20. Mizushima K, Jones PC, Wiseman PJ, Goodenough JB, LixCoO2 (0<x<−1): A new cathode material for batteries of high energy density. Mater. Res. Bull 15, 783–789 (1980).
21. Kawamata Y et al., Scalable, Electrochemical Oxidation of Unactivated C-H Bonds. J. Am. Chem. Soc 139, 7448–7451 (2017). [PubMed: 28510449]
22. Behr S, Hegemann K, Schimanski H, Froehlich R, Haufe G, Synthesis of γ-lactones from cycloocta-1,5-diene - starting materials for natural-product synthesis. Eur. J. Org. Chem, 3884–3892 (2004).
23. Kirste A, Elsler B, Schnakenburg G, Waldvogel SR, Efficient anodic and direct phenolarene C,C cross-coupling: The benign role of water or methanol. J. Am. Chem. Soc 134, 3571–3576 (2012). [PubMed: 22242769]
24. Mihelcic J, Moeller KD, Oxidative Cyclizations: The Asymmetric Synthesis of (−)-Alliacol A. J. Am. Chem. Soc 126, 9106–9111 (2004). [PubMed: 15264845]
25. Ashikari Y, Nokami T, J.-i. Yoshida, Oxidative Hydroxylation Mediated by Alkoxysulfonium Ions. Org. Lett 14, 938–941 (2012). [PubMed: 22273445]
26. Nokami T et al., Iterative Molecular Assembly Based on the Cation-Pool Method. Convergent Synthesis of Dendritic Molecules. J. Am. Chem. Soc 130, 10864–10865 (2008). [PubMed: 18661982]
27. Perkins RJ, Pedro DJ, Hansen EC, Electrochemical Nickel Catalysis for Sp2-Sp3 Cross-Electrophile Coupling Reactions of Unactivated Alkyl Halides. Org. Lett 19, 3755–3758 (2017). [PubMed: 28704055]
28. Sun G, Ren S, Zhu X, Huang M, Wan Y, Direct Arylation of Pyrroles via Indirect Electroreductive C-H Functionalization Using Perylene Bisimide as an Electron-Transfer Mediator. Org. Lett 18, 544–547 (2016). [PubMed: 26800089]
29. Edinger C, Waldvogel SR, Electrochemical deoxygenation of aromatic amides and sulfoxides. Eur. J. Org. Chem 2014, 5144–5148 (2014).
30. Little RD et al., Electroreductive cyclization. Ketones and aldehydes tethered to .alpha.,.beta.-unsaturated esters (nitriles). Fundamental investigations. J. Org. Chem 53, 2287–2294 (1988).

31. Mortensen J, Heinze J, The Electrochemical Reduction of Benzene—First Direct Determination of the Reduction Potential. Angew. Chem. Int. Ed 23, 84–85 (1984).
32. Mousavi MPS, Kashefolgheta S, Stein A, Buhlmann P, Electrochemical Stability of Quaternary Ammonium Cations: An Experimental and Computational Study. J. Electrochem. Soc 163, H74–H80 (2016).
33. Birch AJ, Electrolytic Reduction in Liquid Ammonia. Nature 158, 60 (1946). [PubMed: 20991745]
34. Ninel MA, Zabusova SE, Andrei PT, The Reduction of Organic Compounds by Solvated Electrons Generated Electrochemically. Rus. Chem. Rev 55, 99 (1986).
35. Sternberg Heinz W., Markby R, Wender I, Electrochemical Reduction of the Benzene Ring. J. Electrochem. Soc 110, 425–429 (1963).
36. Benkeser RA, Kaiser EM, Lambert RF, The Selective Reduction of Aromatic Compounds to Dihydro or Tetrahydro Products by an Electrochemical Method. J. Am. Chem. Soc 86, 5272–5276 (1964).
37. Sternberg HW, Markby RE, Wender I, Mohilner DM, Electrolytic generation of solvated electrons and reduction of the benzene ring in ethanol containing hexamethylphosphoramide. J. Am. Chem. Soc 89, 186–187 (1967).
38. Misono A, Osa T, Yamagishi T, Kodama T, Selective electroreduction of the benzene nucleus. J. Electrochem. Soc 115, 266–267 (1968).
39. Dubois J-E, Dodin G, Reaction of the solvated electron and monomeric metal species with toluene and benzene in hexametapol. Hydrogen atom mobility. Tetrahedron Letters 10, 2325–2328 (1969).
40. Avaca LA, Bewick A, Cathodic reduction of anthracene in lithium chloridehexamethylphosphoramide. J. Chem. Soc., Perkin Trans 2, 1709–1712 (1972).
41. Coleman JP, Wagenknecht JH, Reduction of benzene and related compounds in aqueous solution and undivided cells. J. Electrochem. Soc 128, 322–326 (1981).
42. Misra RA, Yadav AK, Reduction of Aromatic Compounds by Solvated Electrons Generated at Cathode. Bull. Chem. Soc. Jpn 55, 347–348 (1982).
43. Kariv-Miller E, Swenson KE, Zemach D, Cathodic Birch reduction of methoxy aromatics and steroids in aqueous solution. J. Org. Chem 48, 4210–4214 (1983).
44. Pasquariello D et al., Electrochemical reduction of benzene by solvated electrons in HMPA-alcohol solutions. J. Phys. Chem 89, 1243–1245 (1985).
45. Del Campo FJ et al., Low-temperature sonoelectrochemical processes. Part 2: Generation of solvated electrons and Birch reduction processes under high mass transport conditions in liquid ammonia. J. Electroanal. Chem 507, 144–151 (2001).
46. Combellas C, Marzouk H, Thiebault A, Electrolytic equipment for reductions in liquid ammonia. J. Appl. Electrochem 21, 267–275 (1991).
47. van Andel-Scheffer PJM, Wonders AH, Barendrecht E, Studies of solvated electrons in LiBr + HMPA solutions using the rotating ring—disk electrode technique: Part 2. The reaction of benzene with solvated electrons. J. Electroanal. Chem 366, 143–146 (1994).
48. Landais Y, Zekri E, Desymmetrization of cyclohexa-1,4-dienes - a straightforward route to cyclic and acyclic polyhydroxylated systems. Eur. J. Org. Chem, 4037–4053 (2002).
49. Liu K, Liu Y, Lin D, Pei A, Cui Y, Materials for lithium-ion battery safety. Science Advances 4, (2018).
50. Coste J, Le-Nguyen D, Castro B, PyBOP®: A new peptide coupling reagent devoid of toxic by-product. Tetrahedron Letters 31, 205–208 (1990).
51. Paddon CA, Ward Jones SE, Bhatti FL, Donohoe TJ, Compton RG, Kinetics and thermodynamics of the Li/Li+ couple in tetrahydrofuran at low temperatures (195–295 K). J. Phys. Org. Chem 20, 677–684 (2007).
52. Burés J, A Simple Graphical Method to Determine the Order in Catalyst. Angew. Chem. Int. Ed 55, 2028–2031 (2016).
53. Wood NCL, Paddon CA, Bhatti FL, Donohoe TJ, Compton RG, Mediated electron transfer from lithium investigated voltammetrically in tetrahydrofuran: why are some mediators more effective reducing reagents than others? J. Phys. Org. Chem 20, 732–742 (2007).

54. Zhou B et al., A High-Performance Li–O2 Battery with a Strongly Solvating Hexamethylphosphoramide Electrolyte and a LiPON-Protected Lithium Anode. Adv. Mat 29, 1701568 (2017).
55. Chusid O, Ein Ely E, Aurbach D, Babai M, Carmeli Y, Electrochemical and spectroscopic studies of carbon electrodes in lithium battery electrolyte systems. Journal of Power Sources 43, 47–64 (1993).
56. Donohoe TJ, House D, Ammonia Free Partial Reduction of Aromatic Compounds Using Lithium Di-tert-butylbiphenyl (LiDBB). J. Org. Chem 67, 5015–5018 (2002). [PubMed: 12098328]
57. Heravi MM, Fard MV, Faghihi Z, Recent Applications of Birch Reduction in Total Synthesis of Natural Products. Curr. Org. Chem 19, 1491–1525 (2015).
58. Yus M, Foubelo F, Reductive opening of heterocycles with lithium metal as a source of functionalized organolithium compounds: synthetic applications. Targets Heterocycl. Syst 6, 136–171 (2002).
59. Luisi R, Capriati V, Editors, Lithium Compounds in Organic Synthesis: From Fundamentals to Applications. (Wiley-VCH Verlag GmbH & Co. KGaA, 2014), pp. 545.
60. Wolckenhauer SA, Rychnovsky SD, Generation and Utility of Tertiary α-Aminoorganolithium Reagents. Org. Lett 6, 2745–2748 (2004). [PubMed: 15281759]
61. Pangborn AB, Giardello MA, Grubbs RH, Rosen RK, Timmers FJ, Safe and Convenient Procedure for Solvent Purification. Organometallics 15, 1518–1520 (1996).
62. Fulmer GR et al., NMR Chemical Shifts of Trace Impurities: Common Laboratory Solvents, Organics, and Gases in Deuterated Solvents Relevant to the Organometallic Chemist. Organometallics 29, 2176–2179 (2010).
63. O'Dea J, Osteryoung J, Lane T, Determining kinetic parameters from pulse voltammetric data. J. Phys. Chem 90, 2761–2764 (1986).
64. Klingler RJ, Kochi JK, Electron-transfer kinetics from cyclic voltammetry. Quantitative description of electrochemical reversibility. J. Phys. Chem 85, 1731–1741 (1981).
65. Nicholson RS, Shain I, Theory of stationary electrode polarography. Single scan and cyclic methods applied to reversible, irreversible, and kinetic systems. Anal. Chem 36, 706–723 (1964).
66. Wagner CD; Naumkin AV; Kraut-Vass A; Allison JW; Powell CJ Jr., J. R. R., NIST X-ray Photoelectron Spectroscopy Database. NIST Standard Reference Database 20, Version 3.2 (Web Version) 2000.
67. Gaussian 09, Revision A.02, Frisch J, Trucks GW, Schlegel HB, Scuseria GE, Robb MA, Cheeseman JR, Scalmani G, Barone V, Mennucci B, Petersson GA, Nakatsuji H, Caricato M, Li X, Hratchian HP, Izmaylov AF, Bloino J, Zheng G, Sonnenberg JL, Hada M, Ehara M, Toyota K, Fukuda R,Hasegawa J, Ishida M, Nakajima T, Honda Y, Kitao O, Nakai H, Vreven T, Montgomery JA Jr., Peralta JE, Ogliaro F, Bearpark M, Heyd JJ, Brothers E, Kudin KN, Staroverov VN, Kobayashi R, Normand J, Raghavachari K, Rendell A, Burant JC, Iyengar SS, Tomasi J, Cossi M, Rega N, Millam JM, Klene M, Knox JE, Cross JB, Bakken V, Adamo C, Jaramillo J, Gomperts R, Stratmann RE, Yazyev O, Austin AJ, Cammi R, Pomelli C, Ochterski JW, Martin RL, Morokuma K, Zakrzewski VG, Voth GA, Salvador P, Dannenberg JJ, Dapprich S, Daniels AD, Farkas Ö, Foresman JB, Ortiz JV, Cioslowski J, and Fox DJ, Gaussian, Inc., Wallingford CT, 2009
68. Becke AD, A new mixing of Hartree-Fock and local-density-functional theories. J. Chem. Phys 98, 1372–1377 (1993).
69. Becke AD, Density-functional thermochemistry. III. The role of exact exchange. J. Chem. Phys 98, 5648–5652 (1993).
70. Lee C, Yang W, Parr RG, Development of the Colle-Salvetti correlation-energy formula into a functional of the electron density. Phys. Rev. B: Condens. Matter 37, 785–789 (1988). [PubMed: 9944570]
71. Ditchfield R, Hehre WJ, Pople JA, Self-consistent molecular-orbital methods. IX. Extended Gaussian-type basis for molecular-orbital studies of organic molecules. J. Chem. Phys 54, 724–728 (1971).
72. Hariharan PC, Pople JA, Accuracy of AHn equilibrium geometries by single determinant molecular orbital theory. Mol. Phys 27, 209–214 (1974).

73. Krishnan R, Binkley JS, Seeger R, Pople JA, Self-consistent molecular orbital methods. XX. A basis set for correlated wave functions. J. Chem. Phys 72, 650–654 (1980).
74. Bard AJ, Faulkner LR, Electrochemical methods: Fundamentals and Applications (John Wiley and Sons, New York, ed. 2, 2001). Kinetics of Electrode Reactions (2001).
75. Chaban VV, Prezhdo OV, Electron Solvation in Liquid Ammonia: Lithium, Sodium, Magnesium, and Calcium as Electron Sources. J. Phys. Chem. B 120, 2500–2506 (2016). [PubMed: 26886153]
76. Janesko BG, Scalmani G, Frisch MJ, Quantifying solvated electrons' delocalization. Phys. Chem. Chem. Phys 17, 18305–18317 (2015). [PubMed: 25994586]
77. Atwood JL et al., Neutral and anionic silylmethyl complexes of Group IIIb and lanthanoid metals; the x-ray crystal and molecular structure of [Li(thf)4][Yb[CH(SiMe3)2]3Cl] (thf = tetrahydrofuran). J. Chem. Soc., Chem. Commun, 140–142 (1978).
78. Eaborn C, Hitchcock PB, Smith JD, Sullivan AC, Crystal structure of the tetrahydrofuran adduct of tris(timethylsilyl)methyllithium, [Li(THF)4][Li[C(SiMe3)3]2], an ate derivative of lithium. J. Chem. Soc., Chem. Commun, 827–828 (1983).
79. Eaborn C, Hitchcock PB, Smith JD, Sullivan AC, Preparation and crystal structure of the argentate complex [Li(tetrahydrofuran)4][Ag[C(SiMe3)3]2]. J. Chem. Soc., Chem. Commun, 870–871 (1984).
80. Edwards PG, Gellert RW, Marks MW, Bau R, Preparation and structure of the phenylcopper ([Cu5(C6H5)6]-) anion. J. Am. Chem. Soc 104, 2072–2073 (1982).
81. Reich HJ, Borst JP, Dykstra RR, Green PD, A nuclear magnetic resonance spectroscopic technique for the characterization of lithium ion pair structures in THF and THF/HMPA solution. J. Am. Chem. Soc 115, 8728–8741 (1993).
82. Kresse G, Furthmueller J, Efficient iterative schemes for ab initio total-energy calculations using a plane-wave basis set. Phys. Rev. B: Condens. Matter 54, 11169–11186 (1996). [PubMed: 9984901]
83. Kresse G, Hafner J, Ab initio molecular-dynamics simulation of the liquid-metal-amorphous-semiconductor transition in germanium. Phys. Rev. B: Condens. Matter 49, 14251–14269 (1994). [PubMed: 10010505]
84. Moroni EG, Kresse G, Hafner J, Furthmuller J, Ultrasoft pseudopotentials applied to magnetic Fe, Co, and Ni: From atoms to solids. Phys. Rev. B: Condens. Matter 56, 15629–15646 (1997).
85. Perdew JP, Ernzerhof M, Burke K, Rationale for mixing exact exchange with density functional approximations. J. Chem. Phys 105, 9982–9985 (1996).
86. Bloechl PE, Projector augmented-wave method. Phys. Rev. B: Condens. Matter 50, 17953–17979 (1994). [PubMed: 9976227]
87. Kresse G, Joubert D, From ultrasoft pseudopotentials to the projector augmented-wave method. Phys. Rev. B: Condens. Matter Mater. Phys 59, 1758–1775 (1999).
88. Grimme S, Antony J, Ehrlich S, Krieg H, A consistent and accurate ab initio parametrization of density functional dispersion correction (DFT-D) for the 94 elements H-Pu. J. Chem. Phys 132, 154104/154101–154104/154119 (2010). [PubMed: 20423165]
89. Henkelman G, Jonsson H, A dimer method for finding saddle points on high dimensional potential surfaces using only first derivatives. J. Chem. Phys 111, 7010–7022 (1999).
90. Henkelman G, Jonsson H, Improved tangent estimate in the nudged elastic band method for finding minimum energy paths and saddle points. J. Chem. Phys 113, 9978–9985 (2000).
91. Henkelman G, Uberuaga BP, Jonsson H, A climbing image nudged elastic band method for finding saddle points and minimum energy paths. J. Chem. Phys 113, 9901–9904 (2000).
92. Filhol J-S, Neurock M, Elucidation of the electrochemical activation of water over Pd by first principles. Angew. Chem., Int. Ed 45, 402–406 (2006).
93. Taylor CD, Wasileski SA, Filhol J-S, Neurock M, First principles reaction modeling of the electrochemical interface: Consideration and calculation of a tunable surface potential from atomic and electronic structure. Phys. Rev. B: Condens. Matter Mater. Phys 73, 165402/165401–165402/165416 (2006).
94. Chen LD, Urushihara M, Chan K, Noerskov JK, Electric Field Effects in Electrochemical CO2 Reduction. ACS Catal. 6, 7133–7139 (2016).

95. Henkelman G, Arnaldsson A, Jónsson H, A fast and robust algorithm for Bader decomposition of charge density. Comput. Mat. Sci 36, 354–360 (2006).

96. Menzek A, Karakaya MG, Kaya AA, Reductions of benzene derivatives whose benzylic positions bear oxygen atoms under mild conditions. Helv. Chim. Acta 91, 2299–2307 (2008).

97. Birch AJ, Mantsch HH, Reductions of acridine by metal-ammonia solutions. Aust. J. Chem 22, 1103–1104 (1969).

98. Petrier C, Suslick K, Ultrasound-enhanced reactivity of calcium in the reduction of aromatic hydrocarbons. Ultrason. Sonochem 7, 53–61 (2000). [PubMed: 10769871]

99. Matsuda I, Shibata M, Sato S, Izumi Y, Cyclo-codimerization of 1,3-butadiene derivatives with non-activated terminal acetylenes catalyzed by a cationic rhodium(I) complex. Tetrahedron Lett. 28, 3361–3362 (1987).

100. Monti SA, Chen S-C, Yang Y-L, Yuan S-S, Bourgeois OP, Rearrangement approaches to polycyclic skeletons. 1. Bridgehead-substituted bicyclo[3.2.1]octene derivatives from bicyclo[2.2.2]octene precursors. J. Org. Chem 43, 4062–4069 (1978).

101. Ley SV et al., A highly convergent total synthesis of the spiroacetal macrolide (+)-milbemycin β1. Tetrahedron 45, 7161–7194 (1989).

102. Cheung FK, Hayes AM, Hannedouche J, Yim ASY, Wills M, "Tethered" Ru(II) Catalysts for Asymmetric Transfer Hydrogenation of Ketones. J. Org. Chem 70, 3188–3197 (2005). [PubMed: 15822981]

103. Zhu YJ et al., Efficient construction of bioactive trans-5A5B6C spirolactones via bicyclo[4.3.0] α-hydroxy ketones. Org. Biomol. Chem 16, 1163–1166 (2018). [PubMed: 29369320]

104. Takenaka N, Chen J, Captain B, Sarangthem RS, Chandrakumar A, Helical Chiral 2-Aminopyridinium Ions: A New Class of Hydrogen Bond Donor Catalysts. J. Am. Chem. Soc 132, 4536–4537 (2010). [PubMed: 20232867]

105. Cavdar H, Saracoglu N, A new approach for the synthesis of 2-substituted indole derivatives via Michael type adducts. Tetrahedron 61, 2401–2405 (2005).

106. Remers WA, Gibs GJ, Pidacks C, Weiss MJ, Reduction of nitrogen heterocycles by lithium in liquid ammonia. III. Indoles and quinolines. J. Org. Chem 36, 279–284 (1971).

107. Remers WA, Gibs GJ, Pidacks C, Weiss MJ, Ring selectivity in the reduction of certain indoles and quinolines by lithium and methanol in liquid ammonia. J. Am. Chem. Soc 89, 5513–5514 (1967).

108. Ashmore JW, Helmkamp GK, Improved procedure for the Birch reduction of indole and carbazole. Org. Prep. Proced. Int 8, 223–225 (1976).

109. Wakita H et al., Synthesis of 5,6,7-trinor-4,8-inter-m-phenylene PGI2 and Beraprost. Tetrahedron 55, 2449–2474 (1999).

110. Shabbir S et al., Pd nanoparticles on reverse phase silica gel as recyclable catalyst for Suzuki-Miyaura cross coupling reaction and hydrogenation in water. J. Organomet. Chem 846, 296–304 (2017).

111. Nemoto T, Hayashi M, Xu D, Hamajima A, Hamada Y, Enantioselective synthesis of (R)-Sumanirole using organocatalytic asymmetric aziridination of an α,β-unsaturated aldehyde. Tetrahedron: Asymmetry 25, 1133–1137 (2014).

112. Berk SC, Yeh MCP, Jeong N, Knochel P, Preparation and reactions of functionalized benzylic organometallics of zinc and copper. Organometallics 9, 3053–3064 (1990).

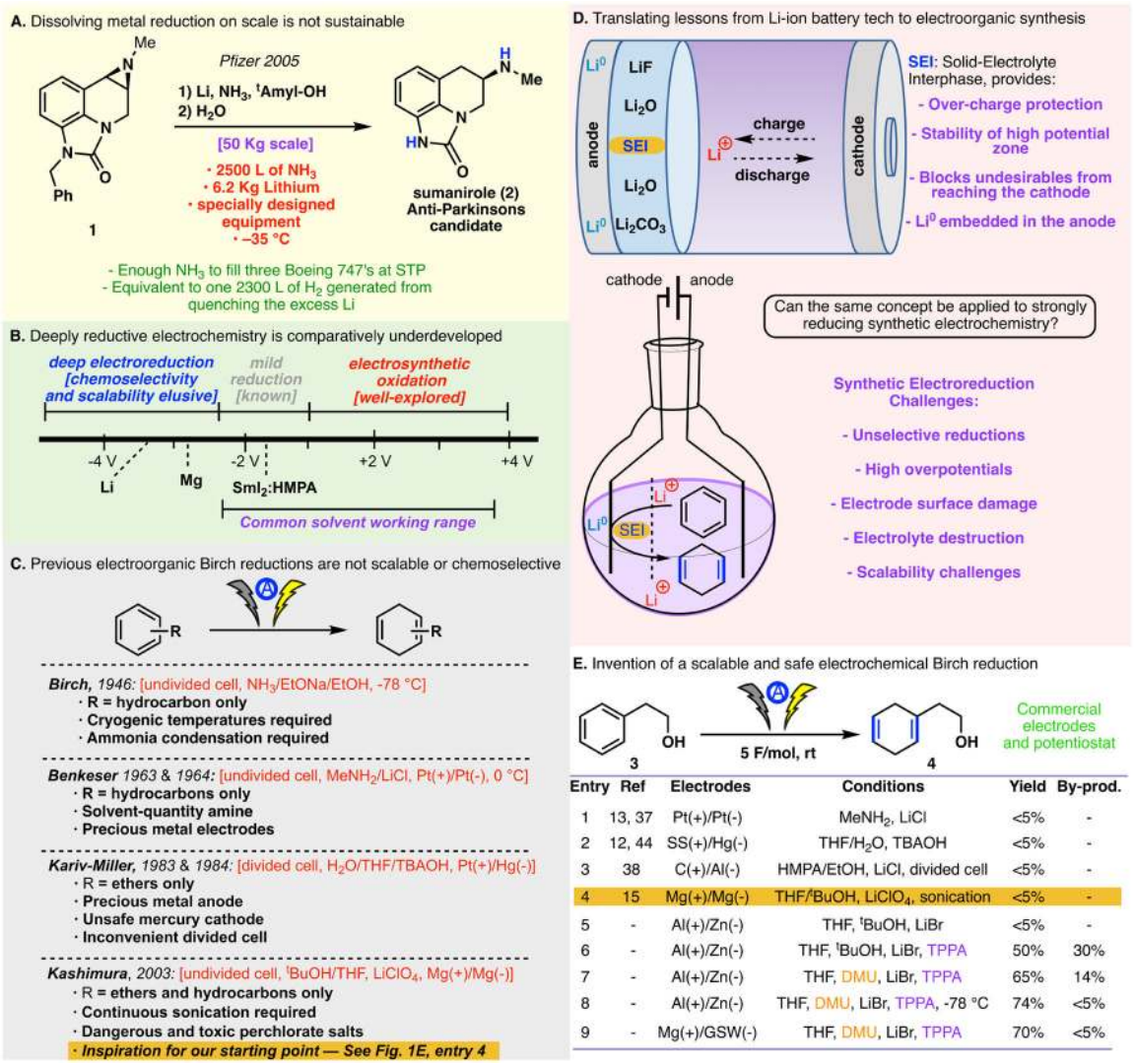

Entry	Ref	Electrodes	Conditions	Yield	By-prod.
1	13, 37	Pt(+)/Pt(-)	$MeNH_2$, LiCl	<5%	-
2	12, 44	SS(+)/Hg(-)	THF/H_2O, TBAOH	<5%	-
3	38	C(+)/Al(-)	HMPA/EtOH, LiCl, divided cell	<5%	-
4	15	Mg(+)/Mg(-)	THF/tBuOH, $LiClO_4$, sonication	<5%	-
5	-	Al(+)/Zn(-)	THF, tBuOH, LiBr	<5%	-
6	-	Al(+)/Zn(-)	THF, tBuOH, LiBr, TPPA	50%	30%
7	-	Al(+)/Zn(-)	THF, DMU, LiBr, TPPA	65%	14%
8	-	Al(+)/Zn(-)	THF, DMU, LiBr, TPPA, -78 °C	74%	<5%
9	-	Mg(+)/GSW(-)	THF, DMU, LiBr, TPPA	70%	<5%

Figure 1: Background and reaction development.

A) Dissolving metal reduction on scale is not sustainable, **B)** Voltage range challenges for reductive electrochemistry, **C)** Electrochemical Birch precedence, **D)** Applying Li-ion battery technology to synthetic electrochemistry, **E)** Optimization of a simple electrochemical alternative to Birch reduction; GSW = Galvanized Steel Wire.

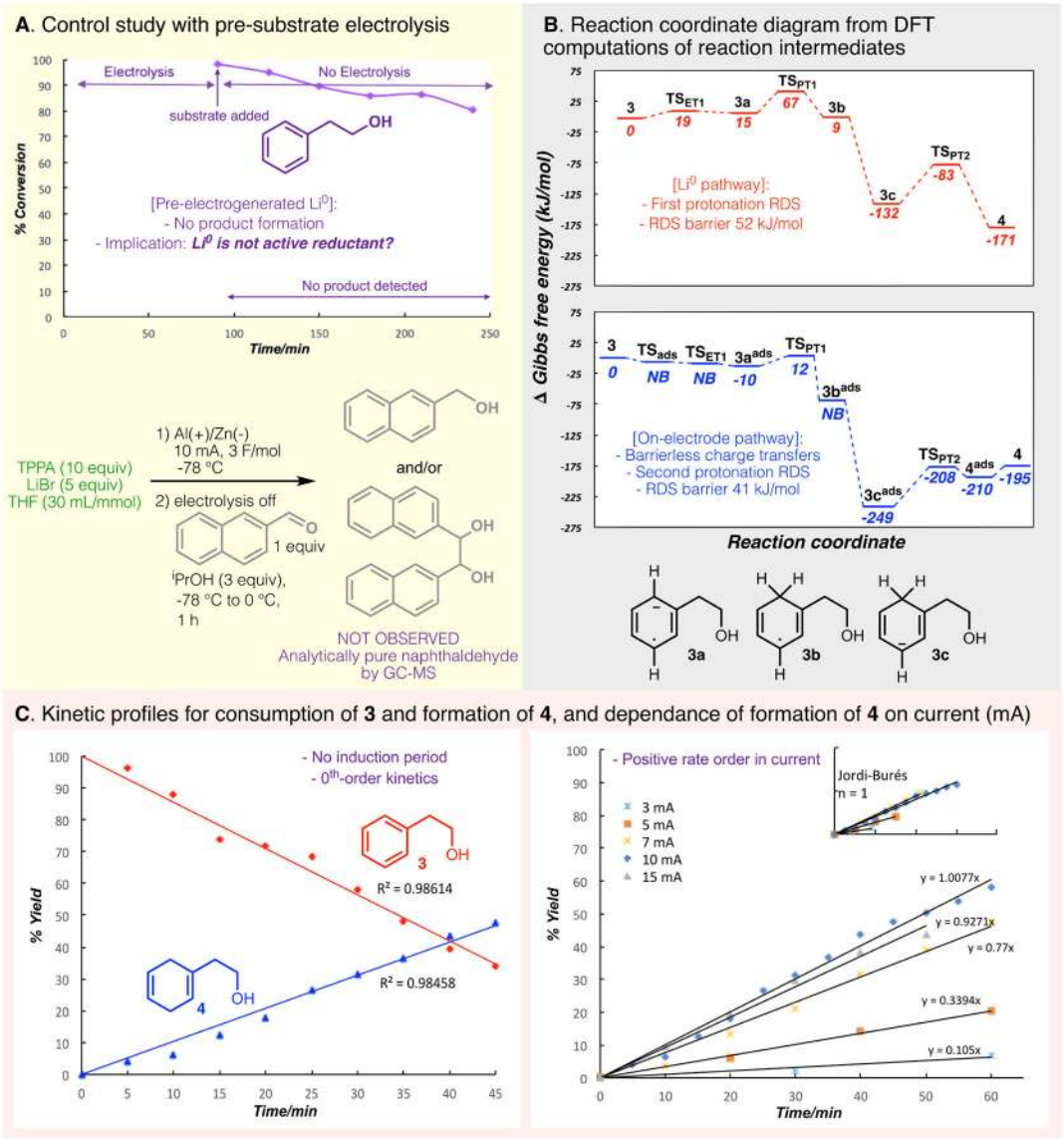

Figure 2. Experimental and computational analysis of the electroreduction of phenethyl alcohol (3). A) Kinetic profile for the relative concentration of arene (**3**) and diene (**4**) in a control experiment involving pre-electrolysis of LiBr solution and Li^0/solvated electrons detection experiment with naphthaldehyde. **B)** Reaction coordinate diagram from DFT computations of reaction intermediates for the reduction of **3** using either solution-phase Li^0 mediation as an electron source (red, top), or a heterogeneous zinc electrode at −2.25 V *vs.* NHE as an electron source (blue, bottom); TSET1 = transition state for electron transfer 1; TS_{PT1} = transition state for proton transfer 1; TS_{PT2} = transition state for proton transfer 2; TS_{ads} = transition state for adsorption; NB = no barrier; *ads* superscripts refer to adsorbed species. **C)** Left: Plot of concentration of **4** generated per time under the standard reaction conditions, indicating zero order kinetics with respect to both the formation of **4** and consumption of **3**; final yield of **4**, 70%. Right: Plot of concentration of **4** generated per time under, varying the

flow of current. Right, inset: Jordi-Burés analysis of current rate dependence, showing current dependence that approximates 1st-order kinetics.

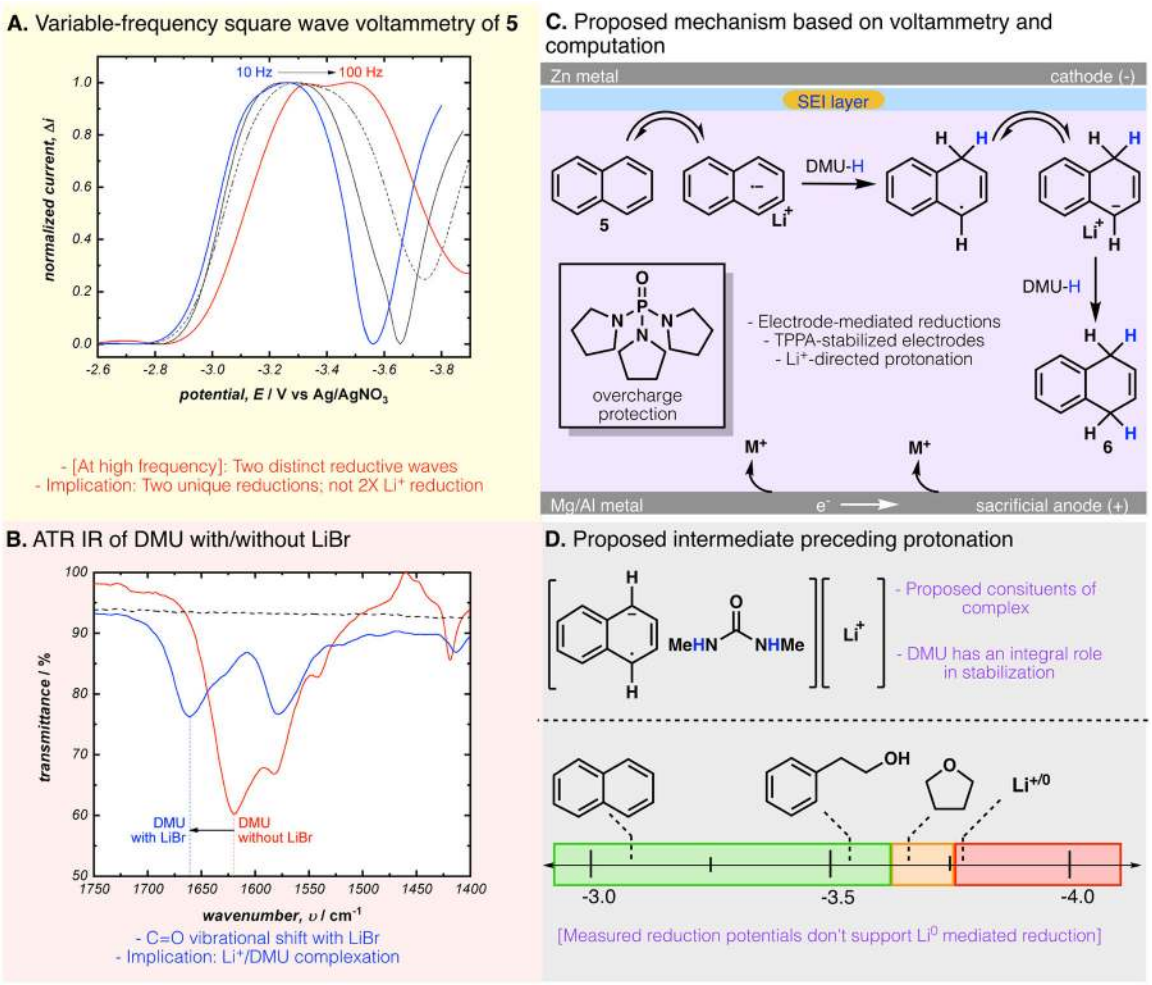

Figure 3. Electrochemical data used to determine the role of various reaction components.

A) Comparative SWVs of 1mM naphthalene (**5**) at 10 (blue) and 100 (red) Hz, **B**) ATR IR of DMU without (red) and with (blue) LiBr, **C**) Scheme of the proposed mechanism of electrochemical Birch reduction, **D**) Proposed intermediate preceding the protonation.

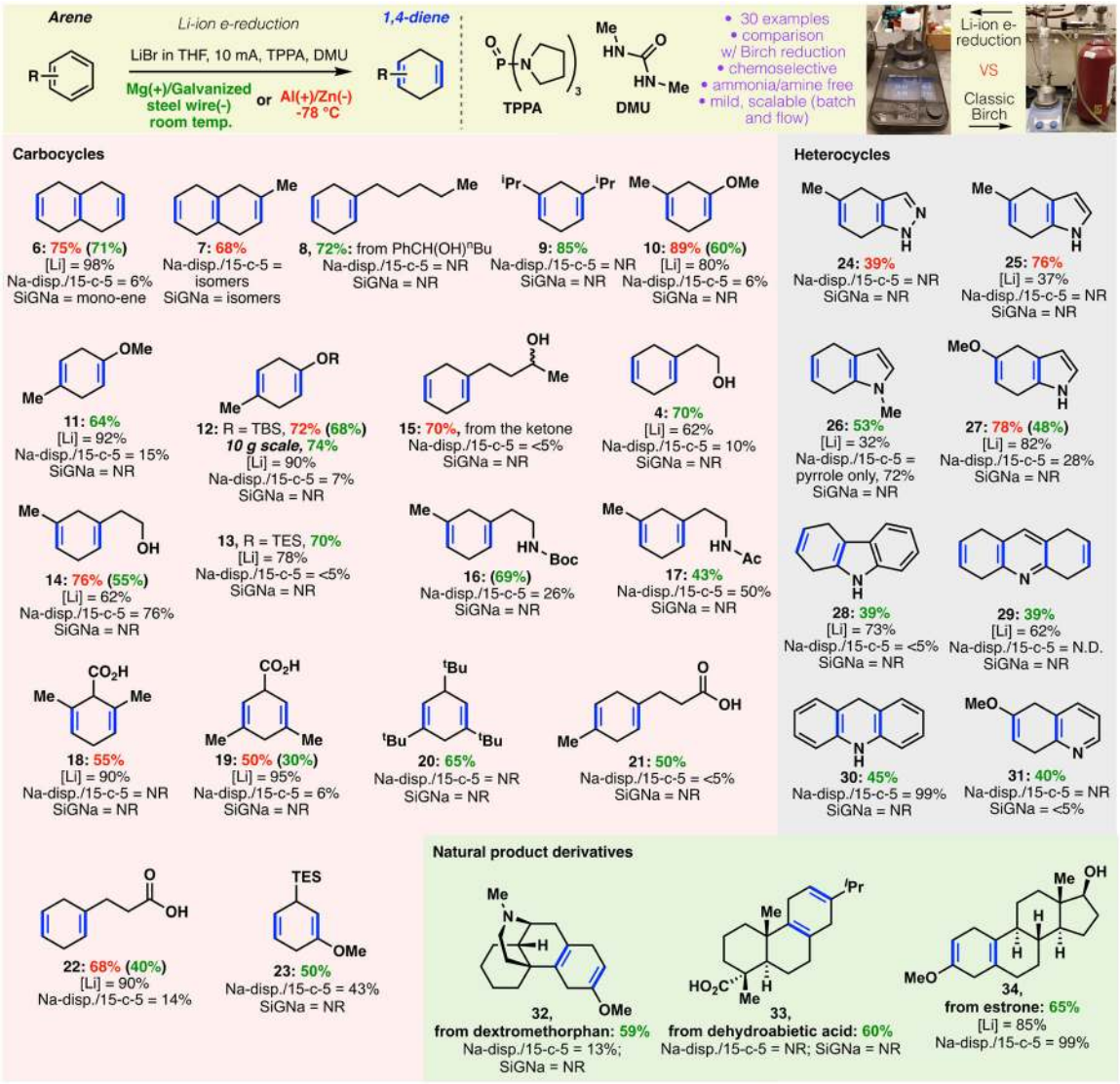

Figure 4: Scope of the electrochemical Birch reaction

, encompassing arenes and heterocycles, and comparison to other modern Birch alternatives. NR = no reaction.

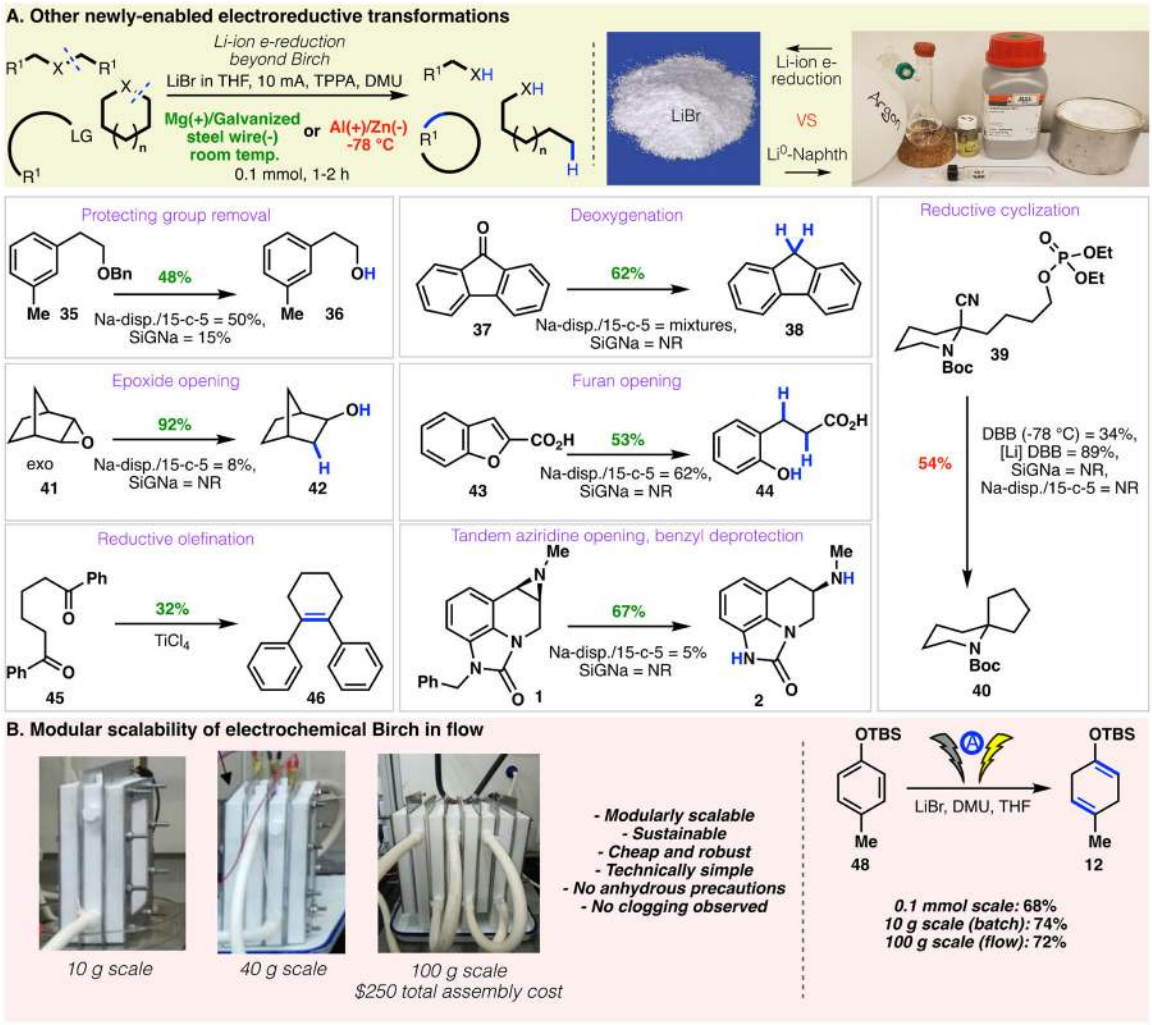

Figure 5. Scope of other reductive electroorganic transformations

A) Scope of the electrochemical reduction in a variety of other reactions, **B)** Modular scaleup of Birch reduction in flow